Nanoscale Res Lett (2007) 2:17–23
DOI 10.1007/s11671-006-9023-7

NANO EXPRESS

Synthesis and characterization of Nb_2O_5@C core-shell nanorods and Nb_2O_5 nanorods by reacting $Nb(OEt)_5$ via RAPET (reaction under autogenic pressure at elevated temperatures) technique

P. P. George · V. G. Pol · A. Gedanken

Published online: 27 October 2006

Abstract The reaction of pentaethoxy niobate, $Nb(OEt)_5$, at elevated temperature (800 °C) under autogenic pressure provides a chemical route to niobium oxide nanorods coated with amorphous carbon. This synthetic approach yielded nanocrystalline particles of Nb_2O_5@C. As prepared Nb_2O_5@C core-shell nanorods is annealed under air at 500 °C for 3 h (removing the carbon coating) results in neat Nb_2O_5 nanorods. According to the TEM measurements, the Nb_2O_5 crystals exhibit particle sizes between 25 nm and 100 nm, and the Nb_2O_5 crystals display rod-like shapes without any indication of an amorphous character. The optical band gap of the Nb_2O_5 nanorods was determined by diffuse reflectance spectroscopy (DRS) and was found to be 3.8 eV.

Keywords Niobia · Nanoparticles · Core-shell structure · Diffused reflection spectroscopy

Introduction

Inorganic nanoparticles with controlled size and shape are technologically important due to the strong correlation between these parameters and their magnetic, opto-electrical, and catalytic properties [1, 2]. Niobium materials have been of special interest due to their opto-electronic properties [3]. In addition, they are used for various important catalytic reactions. The important features of niobium compounds are the promoter effect and the support effect. Niobium oxides remarkably enhance catalytic activity and prolong catalyst life when small amounts are added to known catalysts. Moreover, niobium oxides exhibit a pronounced effect as supports of metal and metal oxide catalysts [4].

The carbon coating of ceramic particles such as Al_2O_3, TiO_2 and MgO, as well as metal particles, are expected to be useful in improving their chemical and physical properties, and are also thought to increase resistance to environmental attack such as corrosion and oxidation. In addition, carbon-coated ceramic particles display improved electrical conductivity. There are a variety of techniques for coating the carbon on nanoparticles, e.g., the electric arc discharging method, which has been used for the production of carbon nanocapsules by coating minute amounts of carbon on metals [5, 6]. However, the reproducibility and homogeneity of these carbon-coated metal particles are not very high, and so their large-scale production is difficult.

Gedanken and co-workers have found a novel method for the carbon coating of a large variety of nanoparticles such as V_2O_5, MoO_3, $MgCNi_3$, $MgCxCo_3$ and WO_3 at elevated temperatures under autogenic pressure, and eventually producing a variety of core-shell nanostructures [7–9]. The technique of this synthetic approach is termed RAPET (reactions under autogenic pressure at elevated temperatures). It does not require any expensive equipment and only involves the simple procedure of adding the precursor to a Letlok cell and heating at 600–1,000 °C under air or under inert atmosphere. Because of its

P. P. George · V. G. Pol · A. Gedanken (✉)
Department of Chemistry and Kanbar Laboratory for Nanomaterials, Bar-Ilan University Center for Advanced Materials Nanotechnology, Bar-Ilan University, Ramat-Gan 52900, Israel
e-mail: gedanken@mail.biu.ac.il

simplicity and ease of application to other ceramics, the RAPET technique is expected to be a one step, efficient process for carbon-coating.

There are various methods for the production of Nb_2O_5 materials [4, 10–13]. Tsuzuki et al. reported on the formation of Nb_2O_5 of 100–1,000 nm by a mechano-chemical synthetic approach [10]. However, the Nb_2O_5 nanoparticles produced were found to be in an aggregated form. The solvothermal approach is another technique for the production of Nb_2O_5 materials [11]. Both techniques have produced amorphous Nb_2O_5 and require further heat treatment to induce crystallization. To overcome these drawbacks, we describe a simple one-step and efficient method for the synthesis of highly crystalline Nb_2O_5 by employing the RAPET method. The advantage of this method over other techniques is that the as-prepared samples are already nanocrystalline in nature. In the present study, carbon-coated crystalline Nb_2O_5 nanorods have been synthesized using a one-step RAPET technique.

Experimental

The synthesis of Nb_2O_5@C core-shell nanorods is carried out by the thermal dissociation of pentaethoxy niobate, $Nb(OEt)_5$, which was purchased from the Aldrich company and used as received. The 3 mL closed vessel cell was assembled from stainless steel Letlok parts (manufactured by the HAM-LET Co., Israel). A 1/2″ union part was plugged from both sides by standard caps as shown in Fig. 1a and b. For the synthesis, 1.5 g of the $Nb(OEt)_5$ was introduced into the cell at room temperature under nitrogen (a nitrogen-filled glove box). The filled cell was closed tightly by the other plug and then placed inside an iron pipe in the middle of the furnace. The temperature was raised at a heating rate of 10 °C/min. The closed-vessel cell was heated at 800 °C for 3 h. The reaction took place under the autogenic pressure of the precursor. The letlok was gradually cooled (~5 h) to room temperature, and after opening, a black powder was obtained. The total yield of the product material was 59% of the total weight of the materials introduced into the cell. [The yield was the final weight of the product relative to the weight of $Nb(OEt)_5$, the starting material]. The synthesis of nanomaterials by the RAPET method required the use of simple equipment, a comparatively low temperature, and a short reaction time, to create pure Nb_2O_5@C nanorods (Sample A). The as-prepared Nb_2O_5@C nanorods were further annealed at 500 °C under air for 3 h. The annealing removes the carbon layer and leads to the formation of white Nb_2O_5 nanorods (Sample B).

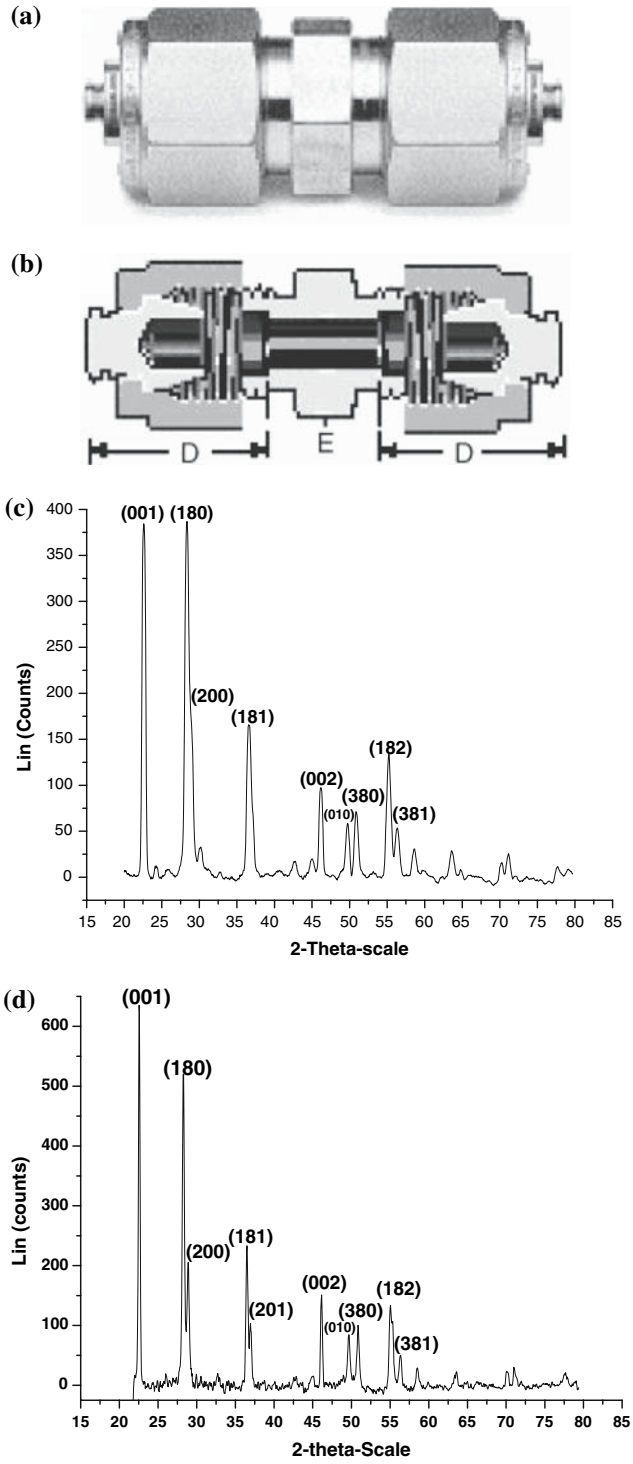

Fig. 1 (**a**) An overview of the Letlok used for the RAPET reaction and (**b**) a cross-section of the Letlok; D: cap, E: union. PXRD pattern of (**c**) the thermally decomposed $Nb(OEt)_5$ at 800 °C under inert atmosphere, (**d**) the thermally decomposed $Nb(OEt)_5$ at 800 °C under inert atmosphere and further annealed at 500 °C under air for 3 h

Characterization

The XRD patterns of samples A and B were recorded using a Bruker D8 diffractometer with Cu Kα radiation. C, H analysis was carried out on an Eager 200 CE instrument and an EA 1110 Elemental Analyzer. The morphologies of the as-prepared sample, and also of the annealed product, were studied by a scanning electron microscope (SEM) coupled with energy dispersive X-ray analysis (EDX). Transmission electron microscopy (TEM) studies were carried out on a JEOL 2000 electron microscope. High-resolution TEM (HRTEM) images were taken using a JEOL 2010 with 200 kV accelerating voltage. Samples for the TEM and HRTEM measurements were obtained by placing a drop of the suspension from the as-sonicated reaction product in ethanol onto a carbon-coated copper grid, followed by drying under air to remove the solvent. EDX studies were carried out on a Jeol micrograph (JEOL 2010 operated at 200 kV). The Olympus BX41 (Jobin Yvon Horiba) Raman spectrometer was employed, using the 514.5 nm line of an Ar ion laser as the excitation source to analyze the nature of the carbon present in Nb_2O_5@C composite. A Micromeritics (Gemini 2375) surface area analyzer was used to measure the surface area of Nb_2O_5@C core-shell nanorods and neat Nb_2O_5 nanorods. The diffuse reflectance spectroscopy (DRS) was carried out using a UV-visible spectrometer (VARIAN CARY 100 Scan).

Results and discussion

Powder X-ray diffraction (PXRD), elemental (C and H) analysis, SEM, HRSEM and EDX analysis

The XRD patterns of the thermally-decomposed $Nb(OEt)_5$ at 800 °C in a closed Letlok cell under inert atmosphere are presented in Fig. 1c. In Fig. 1c, a representative XRD pattern for our as-synthesized carbon-coated niobium oxide nanorods is displayed. All the main peaks can be indexed undisputedly to Nb_2O_5 [powder diffraction file (PDF) no. 00-027-1003]. The degree of carbon graphitization was deduced from the PXRD results. The absence of graphite peaks indicates the possibility that carbon is present only as amorphous carbon. The diffraction peaks at 2θ = 22.6, 28.4, 28.8, 36.6, 37.0, 46.2, 50.0, 50.9, 55.1 and at 56.4° are assigned to (001), (180), (200), (181), (201), (002), (010), (380), (182) and (381) planes of Nb_2O_5, respectively. From the (180) diffraction peak, the average interlayer spacing was calculated as 3.15 Å. The average crystallite size for Nb_2O_5@C and Nb_2O_5 was calculated as ca 28 ± 4 nm using the Debye-Scherrer equation.

When considering the presence of a uniform layer of carbon coated on Nb_2O_5, as will be shown later, the formed product was termed a ''Niobium oxide-carbon'' (NOC) core-shell nanoparticle. To eliminate the carbon, the NOC core-shell was annealed at 500 °C under air. The elemental (C, H, N, S) analysis detected 0% carbon and 0% hydrogen in the product after the annealing process. The diffraction peaks, peak intensities, and cell parameters are in agreement with the diffraction peaks of the crystalline orthorhombic phase of Nb_2O_5 (PDF No. 00-027-1003). The peaks of orthorhombic Nb_2O_5 are narrower compared to those of the Nb_2O_5@C sample, indicating either a crystallite growth due to the sintering of neighboring particles or because of the release of microstrains during the annealing process.

The calculated elemental (wt) percentages of C, H, O and Nb in the $[Nb(OEt)_5]$ precursor are 37.0%, 8.0%, 25.0%, and 29.0%, respectively. We could determine the carbon and hydrogen content in the Nb_2O_5@C sample with an elemental [C, H, N and S] analyzer. The measured amount of carbon in the Nb_2O_5@C sample is 11.64 wt%, while the amount of hydrogen is reduced to 0.14%. Therefore, the final product, Nb_2O_5@C, contains a 33 wt% of the total carbon content that was initially present in the $Nb(OEt)_5$. It is clear that the amount of carbon and hydrogen in the Nb_2O_5@C sample is reduced, as compared with the precursor, because gases such as CO_2, C_xH_y (hydrocarbons) and/or H_2 are formed during the decomposition of the precursor. These gases are liberated as a result of overpressure and upon the opening of the closed Letlok cell [7–9].

The morphologies of the products were observed by SEM, HRSEM, TEM and HRTEM analysis. The morphologies of the Nb_2O_5@C core-shell nanoparticles and the Nb_2O_5 obtained after annealing at 500 °C under air atmosphere are primarily investigated by SEM measurements. Figure 2a and b demonstrates the SEM images of an as-prepared sample, Nb_2O_5@C and neat Nb_2O_5 nanorods, respectively. The sample shows various morphologies, including flakes of different shapes as well defined, rod-shaped particles. The average thickness of the various flakes is ~100 nm. Elemental analysis measurements of the NOC core shell revealed the presence of C in the as-prepared sample. Figure 2b demonstrates the SEM images of neat Nb_2O_5 obtained after annealing the Nb_2O_5@C sample at 500 °C under air. As stated above, the carbon coverage has completely disappeared after the

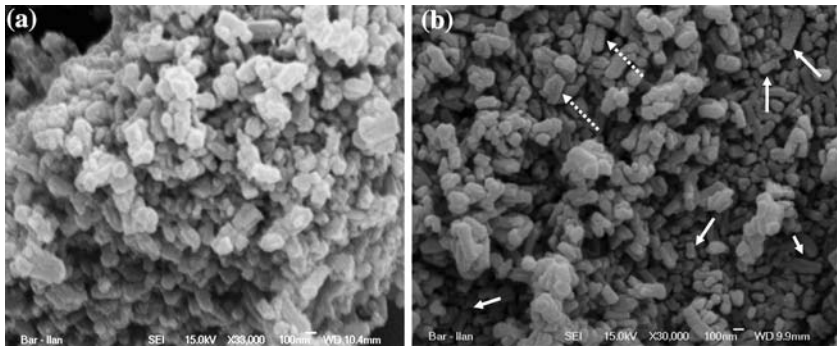

Fig. 2 (**a**) SEM images demonstrating the Nb_2O_5@C core-shell nanoparticles. (**b**) SEM images of neat Nb_2O_5 nanorods obtained after annealing the Nb_2O_5@C core-shell nanorods at 500 °C under air for 3 h. The dashed arrow points to stackings of nanorods. The full arrows point to individual nanorods

annealing treatment. Although many of the flakes are still observed in the SEM picture, the nanorods are also appeared among the annealed particles. The stacking of two or more nanorods (indicated by arrows) is appeared in the SEM images (Fig. 2b). This rod assembly might be due to the sintering of the rods, which occurs upon annealing at 500 °C under air for 3 h. EDX measurements of Nb_2O_5@C core-shell nanorods and neat Nb_2O_5 nanorods indicates the presence of only Nb and oxygen and no other impurities are observed. The composition of the Nb_2O_5@C and neat Nb_2O_5, obtained from EDX analysis, gives Nb/O atomic ratio ~2.5:1 in agreement with Nb_2O_5.

TEM and HRTEM measurements

The structure of the Nb_2O_5@C core shell was further studied by TEM and HRTEM measurements. The TEM image of a few of the rod-shaped Nb_2O_5@C particles obtained by the thermal decomposition of $Nb(OEt)_5$ at 800 °C is illustrated in Fig. 3a. The as-formed Nb_2O_5@C core-shell nanorods have an average thickness of 45–150 nm and lengths of 100–350 nm. Figure 3b demonstrates the HRTEM image of the edge of a single Nb_2O_5@C core-shell nanorod. The image is recorded along the [180] zone. The measured distance between these (180) lattice planes is 0.32 nm, which is very close to the distance between the planes reported in the literature (0.31 nm) for the orthorhombic lattice of the Nb_2O_5 [powder diffraction file (PDF) No. 00-027-1003]. The corresponding selected area electron diffraction (SAED) pattern is demonstrated in Fig. 3c, featuring a single crystal of Nb_2O_5@C core-shell nanoparticles (respective planes are highlighted). In order to identify the composition of core-shell nanorods (HRTEM, Fig. 3a), we have measured a

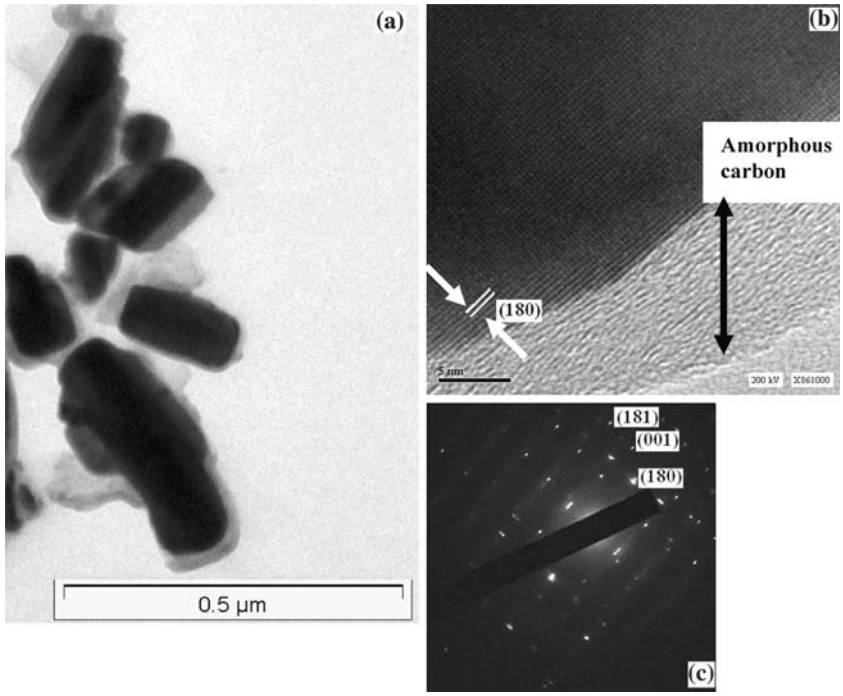

Fig. 3 TEM images of (**a**) Nb_2O_5@C core-shell nanorods, (**b**) a HRTEM image of the edge of a Nb_2O_5@C core-shell nanorod with the plane (180). A uniform amorphous carbon coating of 5–10 nm thickness is clearly seen at the edge of nanorod (marked by black arrow). (**c**) A SAED pattern of Nb_2O_5@C core-shell nanorods (respective planes are highlighted)

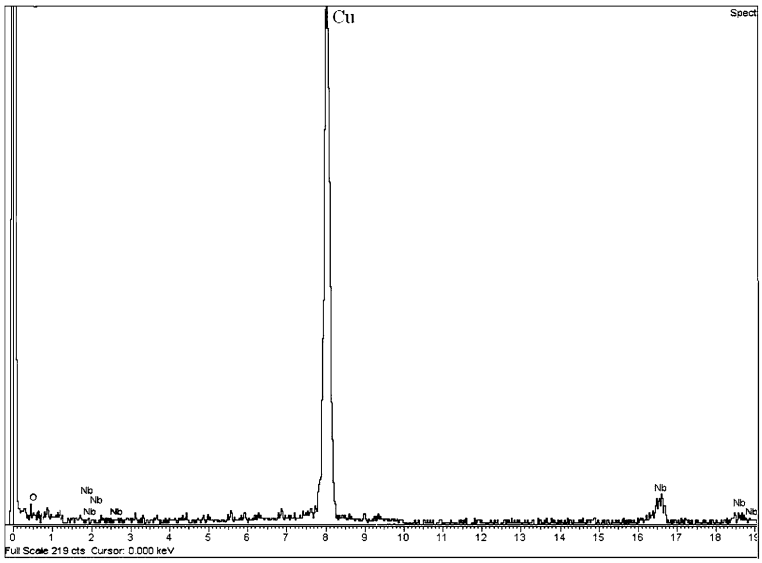

Fig. 4 Selected area EDS analysis of Nb_2O_5@C

selected area EDS analysis of the individual Nb_2O_5@C crystalline particles (Fig. 4). The measurements demonstrate the existence of 69.0 wt% of Nb and 31 wt% of O, which is very close to the theoretical value of Nb_2O_5 (Nb = 69.9 wt% and O = 30 wt%). The carbon peak originates from the carbon shell. The peaks of copper originate from the TEM copper grid.

Figure 5 depicts the TEM image of the morphology of the neat Nb_2O_5 particles. Nanorods are the major structure observed in the picture. They are obtained after annealing the Nb_2O_5@C core-shell nanorods at 500 °C. The neat Nb_2O_5 nanorods have an average thickness of 100 nm and lengths between 100 nm and 300 nm. According to our interpretation, the carbon in the as-prepared Nb_2O_5@C acts as a glue, and it glues together the nanorods of Nb_2O_5, forming flakes of various shapes. Once the glue is removed, the basic shape of the niobia, the nanorods, is exposed.

The results of the Brunauer-Emmett-Teller surface area measurements of the as-prepared Nb_2O_5@C core-shell nanorods prepared under an inert atmosphere and the Nb_2O_5@C core-shell nanorods annealed at 500 °C under air are 14.8 and 14.4 m^2/g, respectively.

We have carried out the optical DRS measurement of the neat Nb_2O_5 nanorods in order to resolve the excitonic or interband (valence conduction band) transitions of Nb_2O_5, which allows us to calculate the band gap. Figure 6 depicts the optical DRS of the Nb_2O_5. An estimate of the optical band gap is obtained using the following equation for a semiconductor [14]:

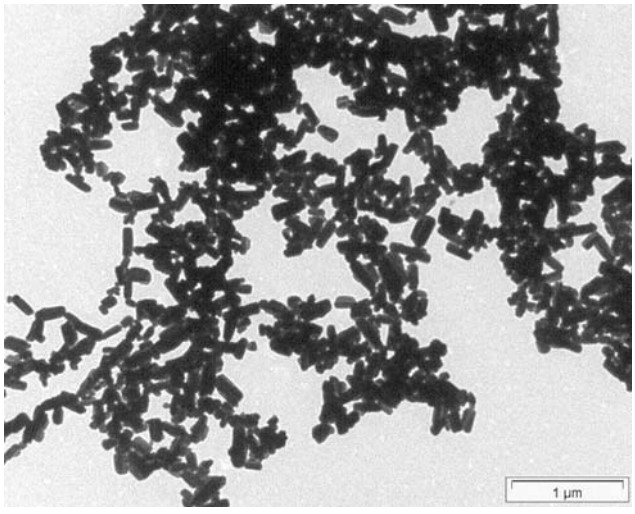

Fig. 5 TEM images of neat Nb_2O_5 nanorods

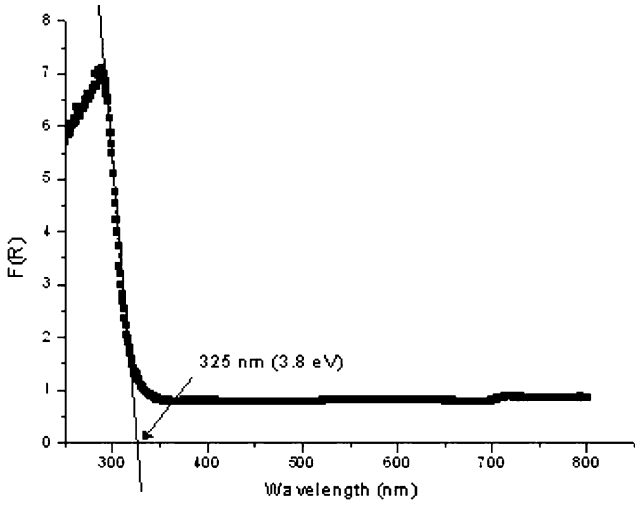

Fig. 6 Diffuse reflectance spectrum (DRS) of Nb_2O_5 nanorod as a function of $F(R)$ versus wavelength (nm)

$$\alpha(v) = A(\hbar v/2 - E_g)^{m/2},$$

where $\hbar = h/\pi$, $\hbar v$ = photon energy, α is the absorption coefficient, and m is dependent on the nature of the transition. For a direct transition, m is equal to 1 or 3, while for an indirect-allowed transition, m is equal to 4 or 6. Since A is proportional to $F(R)$, the Kubelka-Munk function $F(R) = (1 - R)^2/2/R$, the energy intercept of a plot of $(F(R)*hv)^2$ and $(F(R)*hv)^{1/2}$ versus hv yields the $E_{g,\ dir}$ for a direct-allowed transition and the $E_{g,\ ind}$ for an indirect-allowed transition, respectively, when the linear regions are extrapolated to the zero ordinate [14]. Using this method, from the spectrum we calculated the band gap of Nb_2O_5 to be 3.8 eV (325 nm). The value of the band gap energy is shorter than that in the literature, where the bulk band gap is 4.87 eV [15].

We have no explanation for the discrepancy between the bulk value and the band gap measured in this study.

Discussion

The suggested mechanism was based on the obtained analytical data and on a few control experiments, as well as on previously published data. From XRD, EDX, elemental (C, H, N, S) analysis, SEM, HRSEM, TEM, and HRTEM analysis, it was clear that the product, the Nb_2O_5@C core-shell nanorods, were obtained as a result of the thermal dissociation of $Nb(OEt)_5$ under inert atmosphere. A vapor–solid process was presumed to control the formation of the one-dimensional nanostructures, nanotubes, or nanowires [7]. According to our interpretation, the dissociation of $Nb(OEt)_5$ at 800 °C leads to an atomization of the precursor into carbon, hydrogen, oxygen, and perhaps niobium atoms. The niobium and oxygen atoms then react, and upon cooling form a rod-shaped Nb_2O_5 via the fast reactions of ether elimination and β-hydrogen transfer [16]. The occurrence of these reactions, providing oxide nanoparticles in both solution and gas phase thermolysis of metal alkoxides, was earlier demonstrated by us in a series of mechanistic studies [7–9]. Our previous articles, demonstrate that all the products of the dissociation reaction float in the gas phase and solidify immediately after their formation [7]. The question is what solidifies first and what determines the order of the solidification. In the case of the previous RAPET reaction of tetraethyl orthosilicate (TEOS), we could account for the solidification of the carbon [11] by the spherical core, both thermodynamically and kinetically. The present reaction can be explained only on a kinetic basis. Since the boiling and melting points of carbon are much higher than those of the transition metal oxides, thermodynamic carbon would, therefore, tend more easily to become a solid at 800 °C. In other words, from the thermodynamic point of view, carbon would be the first to solidify and form the core, and the Nb_2O_5 would create the shell. However, since the process is kinetically controlled, the opposite occurs. Namely, carbon, having a slower solidification rate, forms the shell layer, and Nb_2O_5 has a much higher solidification rate than carbon for forming the core of the composite. The mechanism for the formation of a similar core-shell structure was discussed in earlier reports [17, 18]. Similar reactions, under the same conditions, were conducted for $VO(OC_2H_5)_3$ and $MoO(OMe)_4$. In both cases, the process is kinetically controlled, and V_2O_3 nanoparticles [17] or MoO_2 nanoparticles [18] showed a higher solidification rate than carbon to form the core of the composite.

Conclusions

Here we present a method for the synthesis of Nb_2O_5@C core-shell nanorods. The presented method is a novel, simple, efficient reaction for the direct preparation of core-shell nanoparticles by a single step process. Anealing the Nb_2O_5@C core-shell nanorods, at 500 °C under air to produce pure Nb_2O_5 nanorods.

Acknowledgements P. P. George thanks the Bar-Ilan Research authority for a post-doctoral fellowship. We are also thankful to Ms. Louise Braverman for editorial assistance. Technical support from Dr. Yuri Koltypin is gratefully acknowledged.

References

1. X. Liu, G. Qiu, X. Li, Nanotechnology **16**, 3035 (2005)
2. T. Ahmad, K.V. Ramanujachary, S.E. Lofland, A.K. Ganguli, J. Nan. Sci. Technol. **5**, 1840 (2005)
3. A. Gargi, G.B. Reddy, J. Mater. Sci: Mater. Elect. **16**, 21 (2005)
4. Y. Chen, I.E. Wachs, J. Catal. **146**, 323 (1994)
5. M. Inagaki, H. Miura, H. Konno, J. Eur. Ceram. Soc. **18**, 1011 (1998)
6. M. Inagaki, Y. Okada, H. Miura, Carbon **37**, 329 (1999)
7. S.V. Pol, V.G. Pol, V.G. Kessler, G.A. Seisenbaeva, M. Sung, S. Asai, A. Gedanken, J. Phys. Chem. B **108**, 6322 (2004)
8. S.V. Pol, V.G. Pol, A. Gedanken, Chem. Eur. J. **10**, 4467 (2004)
9. V.G. Pol, S.V. Pol, A. Gedanken, Y. Goffer, J. Mater. Chem. **14**, 966 (2004)
10. N. Uekawa, T. Kudo, F. Mori, J. Colloid. Interf. Sci. **264**, 378 (2003)
11. T. Tsuzuki, P.G. Mecomick, Mater. Trans. **42**, 8 (2001)
12. O. Friedrichs, F. Aguey-Zinsou, J.R.A. Fernandez, Acta Mater. **54**, 105 (2006)

13. A. Markus, N. Markus, P. Nicola, Colloids Surf. A **250**, 211 (2004)
14. K.V. Luca, S. Djajanti, R.F. Howe, J. Phys. Chem. B **102**, 10650 (1998)
15. G. Agarwal, G.B. Reddy, J. Mater. Sci: Mater. Elect. **16**, 21 (2005)
16. S.V. Pol, V.G. Pol, V.G. Kessler, A. Gedanken, New J. Chem. **30**, 370 (2006)
17. A. Johansson, M. Roman, A.G. Seisenbaeva, L. Kloo, Z. Szabo, V.G. Kessler, J. Chem. Soc. Dalton Trans. 387(2000)
18. S.V. Pol, V.G. Pol, V.G. Kessler, G.A. Seisenbaeva, M.-G. Sung, S. Asai, A. Gedanken, J. Phys. Chem. B **108**, 6322 (2004)